Dynamic analysis of functionally graded plates using a novel FSDT

JL Mantari[+1], EV Granados[ϕ]

[+]Faculty of Mechanical Engineering, Univestity of Enginering and Technology, Av. Cascanueces 2281, Santa Anita, Lima, Perú

[ϕ]Faculty of Mechanical Engineering, National University of Engineering, Av. Túpac Amaru 210, Rimac, Lima, Perú.

Abstract. This paper presents a free vibration analysis of functionally graded plates (FGPs) by using a novel first shear deformation theory (FSDT). This theory contains only four unknowns, with is even less than the classical FSDT. The governing equations for vibrational analysis are derived by employing the principle of Hamilton. These equations are then solved via Navier-type, closed form solutions. The fundamental frequencies are found by solving the eigenvalue problem. The accuracy of the current solutions can be visualized by comparing it with the 3D, classical FSDT and other solutions available in the literature.

---

[1]Corresponding Author email: jmantari@utec.edu.pe Tel: +00511 3540070; Cell: +0051 962224551;

Keywords: Plates; Elasticity; Vibration; Analytical modelling

1. Introduction

Functionally graded materials (FGMs) can be defined as advanced materials having graded transition in mechanical properties, either continuous or in fine, discrete steps, across the interface. This material is produced by mixing two or more materials in a certain volume ratio (commonly ceramic and metal). FGMs have been proposed [1], developed and successfully used in industrial applications since 1980's [2]. These materials were initially

designed as a thermal barrier for aerospace structures and fusion reactors. They are now being developed for general use as structural components subjected to high temperatures. Classical composites structures such as fiber reinforced plastic (FRP) suffer from discontinuity of material properties at the interface of the layers and constituents. Therefore the stress fields in these regions create interface problems and thermal stress concentrations under high temperature environments. Furthermore, large plastic deformation of the interface may trigger the initiation and propagation of cracks in the material [3]. These problems can be decreased by gradually changing the volume fraction of constituent materials and tailoring the material for the desired application. The areas where FGM offer potential improvements and advantages in engineering applications include a reduction of in-plane and transverse through-the-thickness stresses, prevention or reduction of the delamination tendencies in laminated or sandwich structures, improved residual stress distribution, enhanced thermal properties, higher fracture toughness, and reduced stress intensity factors [4].

Many authors have investigated the dynamic behavior of functionally graded plates (FGPs), mostly, by means of both the classical first-order shear deformation theory (FSDT) and the higher-order shear deformation theories (HSDT). In this paper, relevant works on vibrational analysis of FGM based on the classical and modified FSDTs were reviewed and presented in what follows.

Malekzadeh and Alibeygi [5] presented the free vibration analysis of functionally graded (FG) arbitrary straight-sided quadrilateral plates under thermal environment based on the FSDT employing differential quadrature method (DQM). Hosseini et al. [6] analyzed the free vibration of rectangular plates by using the FSDT and exact close-form solution procedure. Zhu et al. [7] presented the free vibration analysis of FGPs using the local Kriging meshless method. The governing equations of free vibration problem are obtained based on the FSDT and the local Petrov-Garlekin formulation.

Natarajan et al. [8] studied the bending and free vibration behavior of functionally graded sandwich plates employed a C^0 8-noded quadrilateral plate element based on HSDT, results based on FSDT were also presented. Valizadeh et al. [9] studied the static and dynamic behaviour of FGPs using a non-uniform rational B-spline based iso-geometric finite element method, where the plate kinematics is based on FSDT. Thai and Choi [10] presented a simple FSDT with four unknowns for bending and free vibration analysis of

FGPs. The authors divided the transverse displacement “w” into bending and shear parts, “w_b” and “w_s”.

In the present paper, the free vibration analysis of functionally graded (FG) sandwich and single plates are studied. The mechanical properties of the plates are assumed to vary in the thickness direction according to a power law distribution or Mori-Tanaka homogenization method in terms of the volume fractions of the constituents. The governing equations of the plates are derived by employing the Hamilton’s principle. These equations are then solved via Navier solution. The fundamental frequencies are found by solving eigenvalue problem. The accuracy of the present code is verified by comparing it with other HSDTs and 3D and quasi-3D solutions available in literature. Although similar results as the classical FSDT are found, the reduced number of unknowns of this theory plays a key importance in the performance. Consequently, the numerical solution may be of paramount interesting for futures works.

2. Analytical modelling

The mathematical model was built to solve both FG sandwich and single plates. Plates of uniform thickness “h”, length “a”, and width “b” are shown in Figure 1a,b. The rectangular Cartesian coordinate system x, y, z, has the plane z = 0, coinciding with the mid-surface of the plates.

The material properties for the single plate (Figure 1a) vary through the thickness with a power law distribution, which is given below (Figure 2a):

$$P_{(z)} = (P_t - P_b)V_{(z)} + P_b \ ,$$

$$V_{(z)} = (\frac{z}{h} + \frac{1}{2})^p \ ,$$

$$-\frac{h}{2} \le z \le \frac{h}{2}. \qquad \text{(1a-c)}$$

where P denotes the effective material property, P_t and P_b denote the property of the top and bottom faces of the plate, respectively, and "p" is the exponent that specifies the material variation profile through the thickness. In addition, the Mori-Tanaka homogenization method was also considered to compute the elastic properties [3].

2.1. Displacement base field

The displacement field of the new theory is given as follows:

$$\begin{aligned}\bar{u}(x,y,z) &= u(x,y) - zk_1\int\theta(x,y)dx,\\ \bar{v}(x,y,z) &= v(x,y) - zk_2\int\theta(x,y)dy,\\ \bar{w}(x,y,z) &= w(x,y).\end{aligned} \tag{2a-c}$$

where $u(x,y)$, $v(x,y)$, $w(x,y)$, and $\theta(x,y)$ are the four unknown displacement functions of middle surface of the plate. The last unknown is a mathematical term that allows obtaining the rotations of the normal to the midplate about the x and y axes (as in the ordinary FSDT). Note that the integrals do not have limits. In the present paper is considered terms with integrals instead of terms with derivatives (see displacement field (2a-c) and [10]). Therefore, to find the values of the coefficients "k_1" and "k_2", some ideas from the paper by Thai and Choi [10] were considered, obtaining:

$$\frac{k_1}{k_2} = \frac{\int \frac{\partial\theta}{\partial x}dy}{\int \frac{\partial\theta}{\partial y}dx} \tag{3}$$

The linear strain expressions derived from the displacement model of Eqs. (2a-c), valid for thin, moderately thick and thick plate under consideration are as follows:

$$\varepsilon_{xx} = \varepsilon^0_{xx} + z\varepsilon^1_{xx}, \qquad \varepsilon_{yy} = \varepsilon^0_{yy} + z\varepsilon^1_{yy}, \qquad \varepsilon_{xy} = \varepsilon^0_{xy} + z\varepsilon^1_{xy},$$

$$\varepsilon_{xz} = \varepsilon^0_{xz}, \qquad \varepsilon_{yz} = \varepsilon^0_{yz}. \tag{4a-e}$$

For the FGP, the stress–strain relationships can be expressed as:

$$\begin{Bmatrix} \sigma_{xx} \\ \sigma_{yy} \\ \tau_{xy} \\ \tau_{xz} \\ \tau_{yz} \end{Bmatrix} = \begin{bmatrix} Q_{11} & Q_{12} & 0 & 0 & 0 \\ Q_{12} & Q_{22} & 0 & 0 & 0 \\ 0 & 0 & Q_{66} & 0 & 0 \\ 0 & 0 & 0 & Q_{55} & 0 \\ 0 & 0 & 0 & 0 & Q_{44} \end{bmatrix} \begin{Bmatrix} \varepsilon_{xx} \\ \varepsilon_{yy} \\ \gamma_{xy} \\ \gamma_{xz} \\ \gamma_{yx} \end{Bmatrix}. \quad (5)$$

in which, $\boldsymbol{\sigma}=\{\sigma_{xx},\sigma_{yy},\tau_{xy},\tau_{xz},\tau_{yz}\}^{\mathrm{T}}$ and $\boldsymbol{\varepsilon}=\{\varepsilon_{xx},\ \varepsilon_{yy},\ \gamma_{xy},\ \gamma_{xz},\ \gamma_{yz}\}^{\mathrm{T}}$ are the stresses and the strain vectors with respect to the plate coordinate system. The Q_{ij} expressions in terms of engineering constants are given below:

$$Q_{11}=Q_{22}=\frac{E}{1-\nu^2}, \quad Q_{12}=\nu Q_{11}, \quad Q_{44}=Q_{55}=Q_{66}=\frac{E}{2(1+\nu)}. \quad (6a\text{-}c)$$

2.2. Hamilton's Principle

The total potential energy of the considered FGP is expressed as:

$$\Pi = U - T \quad (7)$$

where U is the strain energy and T is the kinetic energy. They can be written as:

$$U=\frac{1}{2}\int_V \left[\sigma_{xx}\varepsilon_{xx}+\sigma_{yy}\varepsilon_{yy}+\sigma_{zz}\varepsilon_{zz}+\tau_{yz}\gamma_{yz}+\tau_{xz}\gamma_{xz}+\tau_{xy}\gamma_{xy}\right]dV \quad (8)$$

$$T=\frac{1}{2}\int_V \rho(z)\left[\left(\frac{\partial u}{\partial t}\right)^2+\left(\frac{\partial v}{\partial t}\right)^2+\left(\frac{\partial w}{\partial t}\right)^2\right]dV \quad (9)$$

where $\rho(z)$ is mass density per unit volume.

2.3. Plate governing equations

Using the displacement–strain relations (Eqs. (4a-e) and stress–strain relations (Eq. (5)), and applying integrating by parts and the fundamental lemma of variational calculus and

collecting the coefficients of $\delta u, \delta v, \delta w, \delta\theta$ as in Ref.[14], the motion equations are obtained as:

$$\delta u: \frac{\partial N_1}{\partial x}+\frac{\partial N_6}{\partial y}=I_1\ddot{u}-k_1A'I_2\left(\frac{\partial\ddot{\theta}}{\partial x}\right),$$

$$\delta v: \frac{\partial N_2}{\partial y}+\frac{\partial N_6}{\partial x}=I_1\ddot{v}-k_2B'I_2\left(\frac{\partial\ddot{\theta}}{\partial y}\right),$$

$$\delta w: \frac{\partial N_5}{\partial x}+\frac{\partial^2 N_4}{\partial y}=I_1\ddot{w},$$

$$\delta\theta: k_1M_1+k_2M_2+(k_1A'+k_2B')\frac{\partial^2 M_6}{\partial x\partial y}-k_1A'\frac{\partial N_5}{\partial x}-k_2B'\frac{\partial N_4}{\partial y}=$$

$$k_1A'I_2\left(\frac{\partial\ddot{u}}{\partial x}\right)+k_2B'I_2\left(\frac{\partial\ddot{v}}{\partial y}\right)+I_3\left((k_1A')^2\frac{\partial^2\ddot{\theta}}{\partial x^2}+(k_2B')^2\frac{\partial^2\ddot{\theta}}{\partial y^2}\right) \qquad \text{(10a-d)}$$

where N_i and M_i are the resultants similar to the ones found in Ref. [10].

3. Solution procedure

For the analytical solution of the partial differential equations (Eq. (10a-d)), the Navier method, based on double Fourier series, is used under the specified boundary conditions. Using Navier's procedure, the solution of the displacement variables satisfying the simple supported boundary conditions can be expressed in the following Fourier series:

$$u(x,y)=\sum_{m=1}^{\infty}\sum_{n=1}^{\infty}U_{mn}\cos(\alpha x)\sin(\beta y)e^{i\omega t}, \qquad 0\le x\le a;\ 0\le y\le b$$

$$v(x,y)=\sum_{m=1}^{\infty}\sum_{n=1}^{\infty}V_{mn}\sin(\alpha x)\cos(\beta y)e^{i\omega t}, \qquad 0\le x\le a;\ 0\le y\le b$$

$$w(x,y)=\sum_{m=1}^{\infty}\sum_{n=1}^{\infty}W_{mn}\sin(\alpha x)\sin(\beta y)e^{i\omega t}, \qquad 0\le x\le a;\ 0\le y\le b$$

$$\theta(x,y)=\sum_{m=1}^{\infty}\sum_{n=1}^{\infty}\Theta_{mn}\sin(\alpha x)\sin(\beta y)e^{i\omega t},\qquad 0\le x\le a;\ 0\le y\le b \tag{11a-d}$$

where

$$\alpha=\frac{m\pi}{a},\ \beta=\frac{n\pi}{b}. \tag{12a,b}$$

Substituting Eqs. (11a-d) into Eqs. (10a-d), the following equations are obtained,

$$\left([K]-\omega^2[M]\right)\{\Delta\}=\{0\} \tag{13}$$

where **K** and **M** is stiffness and mass matrices respectively and [Δ**]** is the column vector of coefficients $\{U_{mn}\ \ V_{mn}\ \ W_{mn}\ \ \Theta_{mn}\}^{\mathrm{T}}$.

The elements of K_{ij} and M_{ij} in Eq. (13) are given in Appendix A. The natural frequencies of FGPs can be found from the nontrivial solution of Eq. (13).

4. Numerical results and discussions

In this section the accuracy of the present FSDT which has a displacement field with four unknowns, is evaluated. Numerical examples for free vibration analysis of FG sandwich and single plates with various indexes that specify the material variation profile through the thickness and several values of the side-to-thickness ratio “a/h” and aspect ratio “a/b” are also presented. Typical mechanical properties for metal and ceramics used in the numerical examples are listed in Table 1. In the calculations, both, FG sandwich and single plates are studied. For this study the following relations for presentations of non-dimensional frequencies was utilized:

$$\overline{\beta}=\omega h\sqrt{\rho_M/E_M}$$

$$\hat{\omega}=\omega h\sqrt{\rho_C/E_C}$$

$$\tilde{\beta}=\left(\omega a^2/h\right)\sqrt{\rho_0/E_0}$$

$$\overline{\omega}=\left(\omega a^2/h\right)\sqrt{\rho_C/E_C}$$

$$\rho_0 = 1 kg/m^3$$

$$E_0 = 1 GPa \qquad \text{(14a-f)}$$

4.1 Analysis of FG sandwich and single plates

Results of non-dimensional natural frequencies, $\bar{\beta}$, for simply supported FG square plates are presented in Table 2 for various indexes "*p*" and side-to-thickness ratios "a/h". The materials making up the plate are aluminum at the bottom, and zirconia at the top face (see materials properties in Table 1). The Young's modulus is computed considering the Mori-Tanaka procedure [3]. In this example, the results of the present theory are compared with 3D exact solution presented by Vel and Batra [3], quasi-3D sinusoidal and hyperbolic HSDTs proposed by Neves et al. [12,13], solutions based on HSDT by Mantari et al. [14] and the simple FSDT proposed by Thai and Choi [10]. From this table we can see that the results of non-dimensional natural frequencies obtained from the present theory are close to 3D solution [3] considering a shear correction factor K=5/6. Is worth mentioning that the present results are close to each other, when considering the shear correction factor K = 5/6 and K = 1. The effect of the shear correction factor is less influential in large side-to-thickness ratio "a/h".

Table 3 shows the results of the first two non-dimensional frequencies for simply supported FG square plates. The materials making up the plate are aluminum at the bottom, and alumina at the top face (see materials properties in Table 1). The material properties vary through the thickness with a power law distribution (Eq. (1a-c)). The results of this theory are compared with quasi-3D solutions presented by Matsunaga [11] and solutions based on the simple FSDT by Thai and Choi [10]. The present results are very close to the solutions obtained by Thai and Choi [10] considering the shear correction factor K=5/6, likewise, have a good agreement with the quasi-3D solutions [11]. Again it is noted that the shear correction factor is influential in large side-to-thickness ratio "a/h".

The results of non-dimensional natural frequencies for simply supported FG square sandwich plate are presented in Table 4. In this example three configurations of skin-core-skin thickness (1-1-1, 1-2-1, 2-2-1), several values of indexes "*p*" and three side-to-thickness ratios (a/h={5, 10, 100}) are considered. The material properties vary through the thickness with a power law distribution. The results are compared with solutions based on HSDTs with 9 and 13 unknowns proposed by Natarajan et al. [8], inverse trigonometric HSDT by Nguyen et al.

[15] and the classical FSDT. From this table can observed that results show a good agreement with other theories proposed for comparison when the shear correction factor K = 5/6. When considering a shear correction factor K = 1, the results are close to the solutions of HSDT with 13 unknowns and in some cases even more precise than the results obtained considering the shear correction factor K = 5/6 (see Table 4, for "a/h = 5" and configuration type "2-2-1").

Table 5 shows the results of the lowest four non-dimensional frequencies for simply supported FG rectangular plates. The materials making up the plate are aluminum at the bottom, and alumina at the top face (see materials properties in Table 1). The material properties vary through the thickness with a power law distribution (Eq. (1a-c)). The results of this theory are compared with solutions based on HSDT presented by Mantari et al. [14], solutions based on the simple FSDT by Thai and Choi [10] and the classical FSDT by Hosseini et al.[6]. The present results have a good agreement with the other solutions and are equal to the results obtained by Thai and Choi [10].

The Figures 3 and 4 shows the variation of the non-dimensional natural frequencies of simply supported FG square plates as a function of the index "*p*" and the aspect ratio "a/b", respectively. The curves obtained from this theory are compared with the curves obtained of the HSDT proposed by Mantari et al. [14]. In the calculation process is considered a shear correction factor K=5/6. From these figures can be seen that the resulting curves are very close to the curves obtained by using a HSDT [14]. Consequently, in general, the present theory is successfully validated.

Table 6 present the non-dimensional natural frequencies of FG square sandwich plate. Three configurations of skin (top W)-core (FGM)-skin (Cu), see Table 1. Different thickness (1-1-1, 1-2-1, 2-2-1) and several values of indexes "*p*" for several side-to-thickness ratios (a/h={5, 10, 100}) are considered. Note that the Poisson´s ration were considered constant and equal to 0.31.

As a final remark, it should be stated that the present theory can be further investigated analytically and numerically (by means of both finite element method and meshless). Numerically, the solution procedure perhaps needs a new kind of shape functions. It could be also interesting to see the advantages in terms of computational costs.

5. Conclusions

This paper presents a free vibrational analysis for FG sandwich and single plates using an original FSDT with 4 unknowns. The governing equations are obtained through the Hamilton´s principle. These equations are solved via Navier's method. The fundamental frequencies are found by solving the eigenvalue problem. The results were compared with the solutions of several theories. It is concluded that the results of the present theory with shear correction factor K=5/6 has an excellent agreement with the other theories proposed for comparison. The influence of the shear correction factor K decreases with increasing side-to-thickness ratio "a/h". The present formulation of the displacement field is solved analytically and very close to the classical FSDT results were obtained. Consequently, the authors recommend implementing the numerical solution of this theory.

Appendix A: Definition of Constants in Eq. (13)

A.1. Calculation of $\mathbf{M}_{ij}$:

$$\begin{bmatrix} -I_1 & 0 & 0 & k_1 A' I_2 \alpha \\ 0 & -I_1 & 0 & k_2 B' I_2 \beta \\ & & -I_1 & 0 \\ symm & & & -I_3\left((k_1 A'\alpha)^2 + (k_2 B'\beta)^2\right) \end{bmatrix}$$

A.2. Calculation of $\mathbf{K}_{ij}$:

Calculation of N and M:

$$\begin{bmatrix} (N_1, M_1) \\ (N_2, M_2) \\ (N_6, M_6) \end{bmatrix} = (\text{Aij,Bij}) \begin{bmatrix} -\alpha & 0 & 0 & 0 \\ 0 & -\beta & 0 & 0 \\ \beta & \alpha & 0 & 0 \end{bmatrix} +$$

$$(\text{Bij,Cij}) \begin{bmatrix} 0 & 0 & 0 & -k_1 \\ 0 & 0 & 0 & -k_2 \\ 0 & 0 & 0 & -(k_1 A' + k_2 B')\alpha\beta \end{bmatrix} \qquad \text{(A1)}$$

where i, j = 1, 2, 6

First derivative of N and M with respect to x:

$$\begin{bmatrix} \frac{\partial(N_1, M_1)}{\partial x} \\ \frac{\partial(N_2, M_2)}{\partial x} \\ \frac{\partial(N_6, M_6)}{\partial x} \end{bmatrix} = (\text{Aij,Bij}) \begin{bmatrix} -\alpha^2 & 0 & 0 & 0 \\ 0 & -\alpha\beta & 0 & 0 \\ -\alpha\beta & -\alpha^2 & 0 & 0 \end{bmatrix} +$$

$$(\text{Bij,Cij}) \begin{bmatrix} 0 & 0 & 0 & -k_1\alpha \\ 0 & 0 & 0 & -k_2\alpha \\ 0 & 0 & 0 & (k_1 A' + k_2 B')\alpha^2\beta \end{bmatrix} \qquad \text{(A2)}$$

First derivative of N and M with respect to y:

$$\begin{bmatrix} \frac{\partial(N_1, M_1)}{\partial y} \\ \frac{\partial(N_2, M_2)}{\partial y} \\ \frac{\partial(N_6, M_6)}{\partial y} \end{bmatrix} = (\text{Aij,Bij}) \begin{bmatrix} -\alpha\beta & 0 & 0 & 0 \\ 0 & -\beta^2 & 0 & 0 \\ -\beta^2 & -\alpha\beta & 0 & 0 \end{bmatrix} +$$

$$(\text{Bij,Cij}) \begin{bmatrix} 0 & 0 & 0 & -k_1\beta \\ 0 & 0 & 0 & -k_2\beta \\ 0 & 0 & 0 & (k_1 A' + k_2 B')\alpha\beta^2 \end{bmatrix} \qquad \text{(A3)}$$

Second partial derivative of N and M with respect to x and y:

$$\begin{bmatrix} \frac{\partial^2(N_1, M_1)}{\partial x \partial y} \\ \frac{\partial^2(N_2, M_2^c)}{\partial x \partial y} \\ \frac{\partial^2(N_6, M_6)}{\partial x \partial y} \end{bmatrix} = (\text{Aij,Bij}) \begin{bmatrix} -\alpha^2\beta & 0 & 0 & 0 \\ 0 & -\alpha\beta^2 & 0 & 0 \\ \alpha\beta^2 & \alpha^2\beta & 0 & 0 \end{bmatrix} +$$

$$(\mathrm{Bij,Cij})\begin{bmatrix} 0 & 0 & 0 & -k_1\alpha\beta \\ 0 & 0 & 0 & -k_2\alpha\beta \\ 0 & 0 & 0 & -(k_1A'+k_2B')\alpha^2\beta^2 \end{bmatrix} \quad \text{(A4)}$$

Example to get K(1,j), in Eq. (13):

From the Eqs. (A1) and (A2), $\frac{\partial N_1}{\partial x}$ and $\frac{\partial N_6}{\partial y}$ can be easily obtained and substituted in Eq. (A5).

$$\mathrm{K(1,j)} = \frac{\partial N_1}{\partial x} + \frac{\partial N_6}{\partial y}, \text{ where } \mathrm{j=1,2,\ldots,5.} \quad \text{(A5)}$$

Following the same technique the coefficients associated with **K** can be obtained.

References

[1] M.B. Bever, P.E. Duwez, Gradients in composite materials. Materials Science and Engineering 10 (1972) 1–8.

[2] M. Koizumi, The concept of FGM. Ceramic Transactions 34 (1993) 3-10.

[3] S.S. Vel, R.C. Batra, Three-dimensional exact solution for the vibration of functionally graded rectangular plate. Journal of Sound and Vibration 272 (2004) 703–730.

[4] V. Birman, T. Keil, S. Hosder, Functionally graded materials in engineering, in: S. Thomopoulus, V. Birman, G.M. Genin (Ed.), Structural Interfaces and Attachments in Biology. New York: Springer Science+Business Media New York, 2013, pp.19-41.

[5] P. Malekzadeh, A. Alibeygi Beni, Free vibration of functionally graded arbitrary straight-sided quadrilateral plates in thermal environment. Composite Structures 92 (2010) 2758-2767.

[6] S. Hosseini-Hashemi, M. Fadaee, S.R. Atashipour, A new exact analytical approach for free vibration of Reissner–Mindlin functionally graded rectangular plates. International Journal of Mechanical Sciences 53 (2011) 11–22.

[7] P. Zhu, K.M. Liew, Free vibration analysis of moderately thick functionally graded plates by local Kriging meshless method. Composite Structures 93 (2011) 2925-2944.

[8] S. Natarajan, M. Ganapathi, Bending and vibration of functionally graded material sandwich plates using an accurate theory. Finite Elements in Analysis and Design 57 (2012) 32-42.

[9] N. Valizadeh, S. Natarajan, O.A. Gonzalez, T. Rabczuk, T.Q. Bui, S.P.A. Bordas, NURBS-based finite element analysis of functionally graded plates: Static bending, vibration, buckling and flutter. Composite Structures 99 (2013) 309-326.

[10] H.T. Thai, D.H. Choi, A simple first-order shear deformation theory for the bending and free vibration analysis of functionally graded plates. Composite Structures 101 (2013) 332-340.

[11] H. Matsunaga, Free vibration and stability of functionally graded plates according to a 2-D higher-order deformation theory. Composite Structures 82 (4) (2008) 499–512.

[12] A.M.A. Neves, A.J.M. Ferreira, E. Carrera, C.M.C. Roque, M. Cinefra, R.M.N. Jorge, C.M.M. Soares, A quasi-3D sinusoidal shear deformation theory for the static and free vibration analysis of functionally graded plates. Composites Part B: Engineering 43 (2) (2012) 711–725.

[13] A.M.A. Neves, A.J.M. Ferreira, E. Carrera, M. Cinefra, C.M.C. Roque, R.M.N. Jorge, C.M.M. Soares, A quasi-3D hyperbolic shear deformation theory for the static and free vibration analysis of functionally graded plates. Composite Structures 94 (5) (2012) 1814–1825.

[14] J.L. Mantari, E.V. Granados, C. Guedes Soares, Vibrational analysis of advanced composite plates resting on elastic foundation. Composites Part B: Engineering 66 (2014) 407–419.

[15] V.H. Nguyen, T.K. Nguyen, H.T. Thai, T.P. Vo, A new inverse trigonometric shear deformation theory for isotropic and functionally graded sandwich plates. Composites Part B: Engineering 66 (2014) 233-246.

Table Legends

Table 1. Material properties of the used FG plate and FG sandwich plate.

Table 2. Comparison of non-dimensional natural frequencies $\bar{\beta} = \omega h \sqrt{\rho_M / E_M}$ of Al/ZrO_2 functionally graded square plates.

Table 3. First two non-dimensional frequencies $\hat{\omega} = \omega h \sqrt{\rho_C / E_C}$ of Al/Al_2O_3 functionally graded square plates.

Table 4. Non-dimensional natural frequency $\tilde{\beta} = \left(\omega a^2 / h\right) \sqrt{\rho_0 / E_0}$ of FG square sandwich plates with FG core (Al_2O_3/Al).

Table 5. Comparison of first four non-dimensional frequencies $\bar{\omega} = \left(\omega a^2 / h\right) \sqrt{\rho_C / E_C}$ of Al/Al_2O_3 functionally graded rectangular plate ($b/a = 2$).

Table 6. Non-dimensional natural frequency $\tilde{\beta} = \left(\omega a^2 / h\right) \sqrt{\rho_0 / E_0}$ of FG square sandwich plates with FG core (W/Cu).

Figure Captions

Figure 1. Geometry of functionally graded plates and sandwich plates. (a) FG plate; (b) Sandwich plate with an FG core and isotropic skins (1-2-1)

Figure 2. Functionally graded function $V_C(\bar{z})$ along the thickness of an FG sandwich plate for different values of the index ‘‘p’’; $\bar{z} = \frac{z}{h}$.

Figure 3. Variation of non-dimensional fundamental frequency $\bar{\omega} = \left(\omega a^2 / h\right) \sqrt{\rho_C / E_C}$ of Al/Al_2O_3 functionally graded square plates with power law index “*p*”.

Figure 4. Variation of non-dimensional fundamental frequency $\bar{\omega} = \left(\omega a^2 / h\right)\sqrt{\rho_C / E_C}$ of Al/Al_2O_3 versus the aspect ratio "a/b" of FG square plates (a/h=10).

TABLES

Table 1.

Material	Properties		
	E (GPa)	**ρ (kg/m^3)**	**ν**
Aluminum (Al)	70	2702	0.3
Alumina (Al_2O_3)	380	3800	0.3
Zirconia (ZrO_2)	200	5700	0.3
Cupper (Cu)	85	19300	0.34
Tungsten (W)	410	8900	0.28

Table 2

Theory	p=0		p=1			a/h=5		
	a/h=$\sqrt{10}$	**a/h=10**	**a/h=5**	**a/h=10**	**a/h=20**	**p=2**	**p=3**	**p=5**
Vel and Batra [3]	0.4658	0.0578	0.2192	0.0596	0.0153	0.2197	0.2211	0.2225
Thai and Choi [10]	0.4618	0.0577	0.2173	0.0592	0.0152	0.2189	0.2207	0.2222
Neves et al. [12]	-	-	0.2193	0.0596	0.0153	0.2198	0.2212	0.2225
Neves et al. [13]	-	-	0.2193	0.0596	0.0153	0.2201	0.2216	0.2230
Mantari et al. [14]	0.4624	0.0577	0.2277	0.0619	0.0158	0.2257	0.2263	0.2271
Present (K=1)	**0.4744**	**0.0579**	**0.2204**	**0.0595**	**0.0152**	**0.2221**	**0.2240**	**0.2256**
Present (K=5/6)	**0.4618**	**0.0577**	**0.2173**	**0.0592**	**0.0152**	**0.2189**	**0.2207**	**0.2222**

Table 3

Mode	a/h	Theory	p				
			0	**0.5**	**1**	**4**	**10**
1	2	Thai and Choi [10]	0.9265	0.8062	0.7333	0.6116	0.5644
		Matsunaga [11]	0.9400	0.8233	0.7477	0.5997	0.5460
		Present (K=1)	**0.9673**	**0.8389**	**0.7614**	**0.6365**	**0.5907**
		Present (K=5/6)	**0.9265**	**0.8062**	**0.7333**	**0.6116**	**0.5644**
	5	Thai and Choi [10]	0.2112	0.1805	0.1631	0.1397	0.1324
		Matsunaga [11]	0.2121	0.1819	0.1640	0.1383	0.1306
		Present (K=1)	**0.2142**	**0.1828**	**0.1651**	**0.1416**	**0.1345**
		Present (K=5/6)	**0.2112**	**0.1805**	**0.1631**	**0.1397**	**0.1324**
	10	Thai and Choi [10]	0.0577	0.0490	0.0442	0.0382	0.0366
		Matsunaga [11]	0.0578	0.0492	0.0443	0.0381	0.0364
		Present (K=1)	**0.0579**	**0.0492**	**0.0444**	**0.0384**	**0.0368**
		Present (K=5/6)	**0.0577**	**0.0490**	**0.0442**	**0.0382**	**0.0366**
2	2	Thai and Choi [10]	1.7045	1.4991	1.3706	1.1285	1.0254
		Matsunaga [11]	1.7406	1.5425	1.4078	1.1040	0.9847
		Present (K=1)	**1.8097**	**1.5856**	**1.4455**	**1.1926**	**1.0906**
		Present (K=5/6)	**1.7045**	**1.4991**	**1.3706**	**1.1285**	**1.0254**
	5	Thai and Choi [10]	0.4618	0.3978	0.3604	0.3049	0.2856
		Matsunaga [11]	0.4658	0.4040	0.3644	0.3000	0.2790
		Present (K=1)	**0.4744**	**0.4076**	**0.3688**	**0.3126**	**0.2941**
		Present (K=5/6)	**0.4618**	**0.3977**	**0.3604**	**0.3049**	**0.2856**
	10	Thai and Choi [10]	0.1376	0.1173	0.1059	0.0911	0.0867
		Matsunaga [11]	0.1381	0.1180	0.1063	0.0905	0.0859
		Present (K=1)	**0.1390**	**0.1183**	**0.1068**	**0.0920**	**0.0877**
		Present (K=5/6)	**0.1376**	**0.1173**	**0.1059**	**0.0911**	**0.0867**

Table 4

a/h	Theory	1-1-1				1-2-1			2-2-1		
		0	**0.5**	**1**	**5**	**0.5**	**1**	**5**	**0.5**	**1**	**5**
5	Natarajan et al. [8] (HSDT9)	1.1021	1.1449	1.1639	1.2113	1.1597	1.1884	1.2644	1.1965	1.2350	1.3249
	Natarajan et al. [8] (HSDT13)	1.0893	1.1511	1.1701	1.2162	1.1663	1.1952	1.2712	1.2031	1.2421	1.3312
	Nguyen et al. [15]	1.1147	1.1414	1.1561	1.1996	1.1574	1.1827	1.2569	1.1916	1.2268	1.3160
	FSDT	1.1263	1.1503	1.1642	1.2050	1.1660	1.1880	1.2567	1.1950	1.2299	1.3173
	Present (K=1)	**1.1401**	**1.1630**	**1.1766**	**1.2173**	**1.1797**	**1.2012**	**1.2700**	**1.2079**	**1.2431**	**1.3318**
	Present (K=5/6)	**1.1274**	**1.1512**	**1.1650**	**1.2058**	**1.1670**	**1.1889**	**1.2575**	**1.1958**	**1.2307**	**1.3180**
10	Natarajan et al. [8] (HSDT9)	1.2138	1.2373	1.2506	1.2921	1.2578	1.2785	1.3492	1.2846	1.3216	1.4161
	Natarajan et al. [8] (HSDT13)	1.2087	1.2392	1.2524	1.2935	1.2598	1.2806	1.3513	1.2865	1.3238	1.4180
	Nguyen et al. [15]	1.2172	1.2359	1.2478	1.2883	1.2567	1.2763	1.3466	1.2827	1.3187	1.4130
	FSDT	1.2225	1.2394	1.2509	1.2903	1.2601	1.2786	1.3469	1.2842	1.3201	1.4136
	Present (K=1)	**1.2275**	**1.2438**	**1.2551**	**1.2944**	**1.2649**	**1.2831**	**1.3512**	**1.2887**	**1.3245**	**1.4184**
	Present (K=5/6)	**1.2233**	**1.2400**	**1.2515**	**1.2907**	**1.2608**	**1.2792**	**1.3473**	**1.2848**	**1.3206**	**1.4140**
100	Natarajan et al. [8] (HSDT9)	1.2617	1.2751	1.2854	1.3239	1.2981	1.3148	1.3825	1.3198	1.3559	1.4519
	Natarajan et al. [8] (HSDT13)	1.2616	1.2751	1.2854	1.3239	1.2981	1.3148	1.3825	1.3198	1.3559	1.4519
	Nguyen et al. [15]	1.2617	1.2752	1.2853	1.3238	1.2984	1.3147	1.3824	1.3198	1.3558	1.4518
	FSDT	1.2618	1.2751	1.2854	1.3239	1.2981	1.3148	1.3825	1.3198	1.3559	1.4518
	Present (K=1)	**1.2625**	**1.2758**	**1.2859**	**1.3243**	**1.2993**	**1.3153**	**1.3828**	**1.3203**	**1.3562**	**1.4521**
	Present (K=5/6)	**1.2624**	**1.2758**	**1.2859**	**1.3242**	**1.2993**	**1.3153**	**1.3827**	**1.3203**	**1.3562**	**1.4520**

Table 5

a/h	Mode no. (m,n)	Theory	P						
			0	**0.5**	**1**	**2**	**5**	**8**	**10**
5	1 (1,1)	Hosseini et al. [6]	3.4409	2.9322	2.6473	2.4017	2.2528	2.1985	2.1677
		Thai et al. [10]	3.4409	2.9322	2.6473	2.4017	2.2528	2.1985	2.1677
		Mantari et al. [14]	3.4414	2.9348	2.6476	2.3948	2.2264	2.1691	2.1404
		Present (K=5/6)	**3.4409**	**2.9322**	**2.6473**	**2.4017**	**2.2528**	**2.1985**	**2.1677**
	2 (1,2)	Hosseini et al. [6]	5.2802	4.5122	4.0773	3.6953	3.4492	3.3587	3.3094
		Thai et al. [10]	5.2802	4.5122	4.0773	3.6953	3.4492	3.3587	3.3094
		Mantari et al. [14]	5.2817	4.5183	4.0784	3.6804	3.3922	3.2952	3.2507
		Present (K=5/6)	**5.2802**	**4.5122**	**4.0773**	**3.6953**	**3.4492**	**3.3587**	**3.3094**
	3 (1,3)	Hosseini et al. [6]	8.0710	6.9231	6.2636	5.6695	5.2579	5.1045	5.0253
		Thai et al. [10]	8.0710	6.9231	6.2636	5.6695	5.2579	5.1045	5.0253
		Mantari et al. [14]	8.0759	6.9374	6.2670	5.6388	5.1393	4.9736	4.9045
		Present (K=5/6)	**8.0710**	**6.9231**	**6.2636**	**5.6695**	**5.2579**	**5.1045**	**5.0253**
	4 (2,1)	Hosseini et al. [6]	9.7416	8.6926	7.8711	7.1189	6.5749	5.9062	5.7518
		Thai et al. [10]	10.1089	8.6926	7.8711	7.1189	6.5749	6.3708	6.2683
		Mantari et al. [14]	10.1182	8.7152	7.8774	7.0750	6.4030	6.1817	6.0942
		Present (K=5/6)	**10.1089**	**8.6926**	**7.8711**	**7.1189**	**6.5749**	**6.3708**	**6.2683**
10	1 (1,1)	Hosseini et al. [6]	3.6518	3.0983	2.7937	2.5386	2.3998	2.3504	2.3197
		Thai et al. [10]	3.6518	3.0983	2.7937	2.5386	2.3998	2.3504	2.3197
		Mantari et al. [14]	3.6518	3.0990	2.7937	2.5364	2.3913	2.3409	2.3109
		Present (K=5/6)	**3.6518**	**3.0983**	**2.7937**	**2.5386**	**2.3998**	**2.3504**	**2.3197**
	2 (1,2)	Hosseini et al. [6]	5.7693	4.8997	4.4192	4.0142	3.7881	3.7072	3.6580
		Thai et al. [10]	5.7693	4.8997	4.4192	4.0142	3.7881	3.7071	3.6580
		Mantari et al. [14]	5.7695	4.9015	4.4193	4.0089	3.7676	3.6841	3.6366
		Present (K=5/6)	**5.7693**	**4.8997**	**4.4192**	**4.0142**	**3.7881**	**3.7071**	**3.6580**
	3 (1,3)	Hosseini et al. [6]	9.1876	7.8145	7.0512	6.4015	6.0247	5.8887	5.8086
		Thai et al. [10]	9.1876	7.8145	7.0512	6.4015	6.0247	5.8887	5.8086
		Mantari et al. [14]	9.1883	7.8191	7.0517	6.3884	5.9749	5.8329	5.7568
		Present (K=5/6)	**9.1876**	**7.8144**	**7.0512**	**6.4015**	**6.0247**	**5.8887**	**5.8086**
	4 (2,1)	Hosseini et al. [6]	11.8310	10.0740	9.0928	8.2515	7.7505	7.5688	7.4639
		Thai et al. [10]	11.8307	10.0737	9.0928	8.2515	7.7505	7.5688	7.4639
		Mantari et al. [14]	11.8319	10.0813	9.0936	8.2306	7.6707	7.4795	7.3811
		Present (K=5/6)	**11.8307**	**10.0736**	**9.0928**	**8.2515**	**7.7505**	**7.5688**	**7.4639**
20	1 (1,1)	Hosseini et al. [6]	3.7123	3.1456	2.8352	2.5777	2.4425	2.3948	2.3642
		Thai et al. [10]	3.7123	3.1456	2.8352	2.5777	2.4425	2.3948	2.3642
		Mantari et al. [14]	3.7123	3.1457	2.8352	2.5771	2.4402	2.3922	2.3619

		Present (K=5/6)	**3.7123**	**3.1455**	**2.8352**	**2.5777**	**2.4425**	**2.3948**	**2.3643**
	2 (1,2)	Hosseini et al. [6]	5.9198	5.0175	4.5228	4.1115	3.8939	3.8170	3.7681
		Thai et al. [10]	5.9199	5.0175	4.5228	4.1115	3.8939	3.8170	3.7681
		Mantari et al. [14]	5.9199	5.0178	4.5228	4.1100	3.8882	3.8106	3.7621
		Present (K=5/6)	**5.9199**	**5.0173**	**4.5228**	**4.1115**	**3.8939**	**3.8170**	**3.7682**
	3 (1,3)	Hosseini et al. [6]	9.5668	8.1121	7.3132	6.6471	6.2903	6.1639	6.0843
		Thai et al. [10]	9.5669	8.1121	7.3132	6.6471	6.2903	6.1639	6.0843
		Mantari et al. [14]	9.5670	8.1131	7.3133	6.6432	6.2756	6.1472	6.0689
		Present (K=5/6)	**9.5669**	**8.1118**	**7.3132**	**6.6471**	**6.2903**	**6.1639**	**6.0843**
	4 (2,1)	Hosseini et al. [6]	12.4560	10.5660	9.5261	8.6572	8.1875	8.0207	7.9166
		Thai et al. [10]	12.4562	10.5657	9.5261	8.6572	8.1875	8.0207	7.9165
		Mantari et al. [14]	12.4564	10.5674	9.5262	8.6508	8.1628	7.9927	7.8906
		Present (K=5/6)	**12.4562**	**10.5653**	**9.5261**	**8.6572**	**8.1875**	**8.0207**	**7.9166**

Table 6

a/h	Theory	1-1-1			1-2-1			2-2-1		
		0.5	1	5	0.5	1	5	0.5	1	5
5	Present (K=1)	0.612	0.608	0.608	0.628	0.618	0.618	0.609	0.612	0.628
	Present (K=5/6)	0.605	0.601	0.601	0.621	0.612	0.610	0.602	0.605	0.619
10	Present (K=1)	0.650	0.647	0.651	0.668	0.659	0.664	0.649	0.655	0.679
	Present (K=5/6)	0.648	0.645	0.649	0.666	0.657	0.661	0.647	0.653	0.676
100	Present (K=1)	0.665	0.662	0.668	0.684	0.675	0.682	0.665	0.672	0.699
	Present (K=5/6)	0.665	0.662	0.668	0.684	0.675	0.682	0.665	0.672	0.699

Figures

Figure 1.

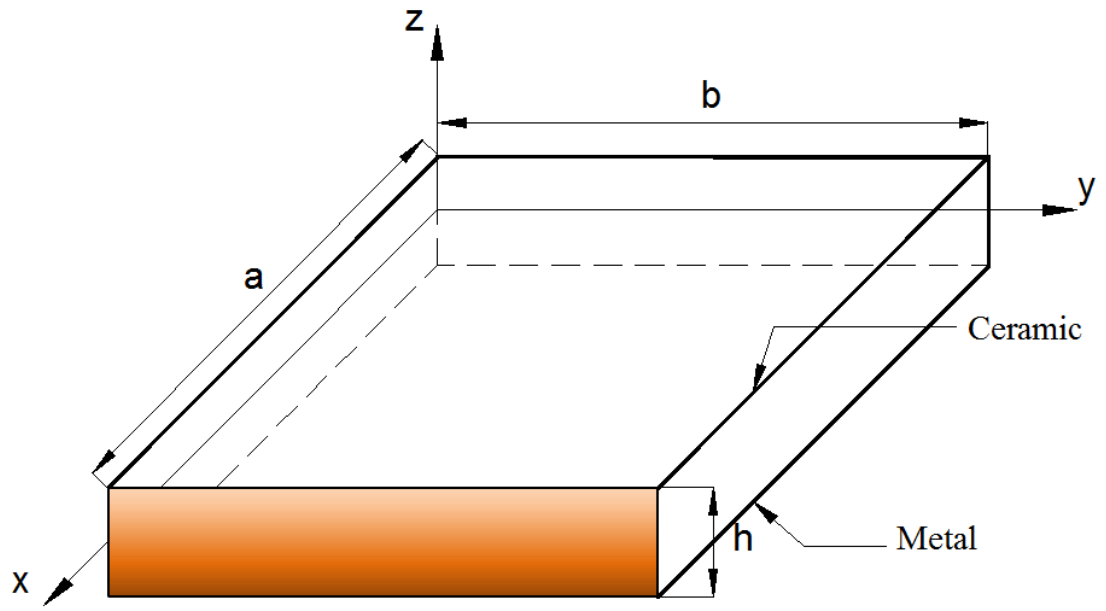

(a) FG plate

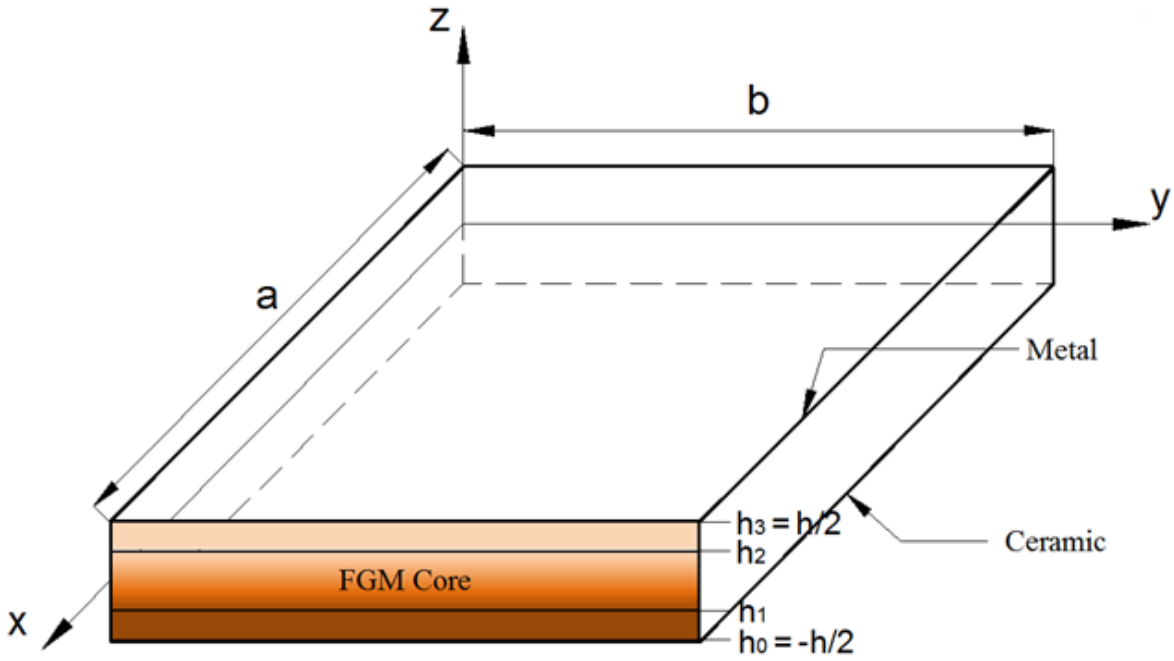

(b) Sandwich plate with an FG core and isotropic skins.

Figure 2.

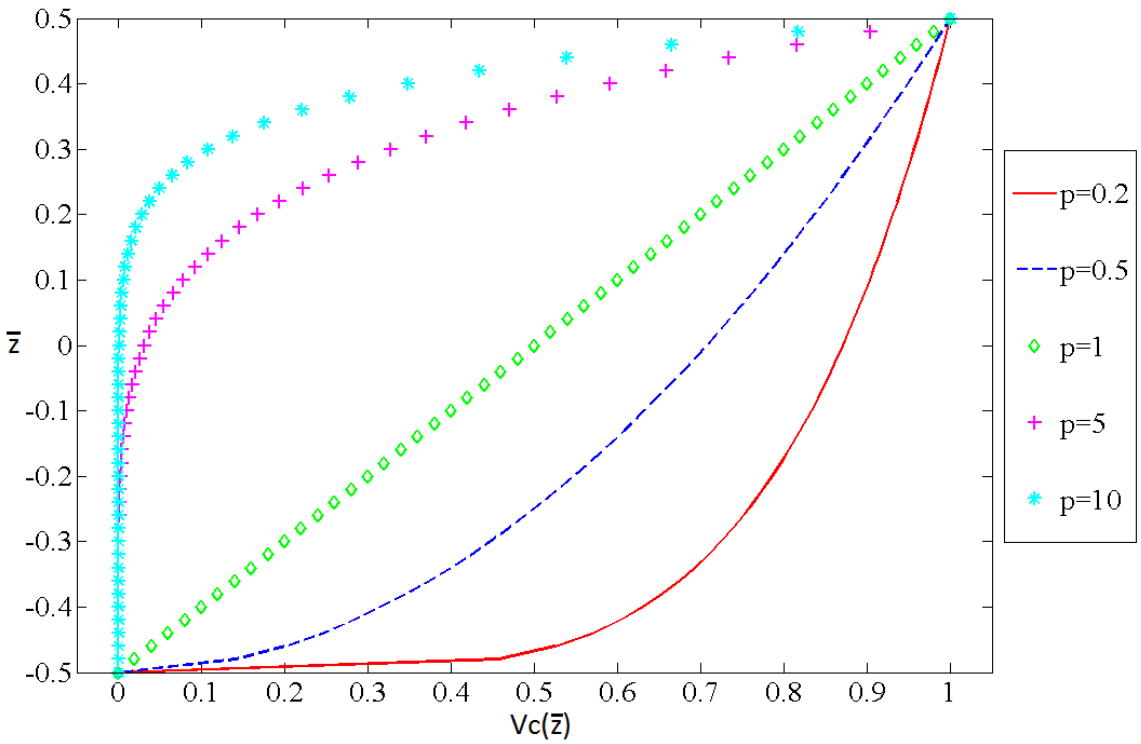
0.5
0.4
0.3
0.2
0.1
0
-0.1
-0.2
-0.3
-0.4
-0.5
z̄
0
0.1
0.2
0.3
0.4
0.5
0.6
0.7
0.8
0.9
1
Vc(z̄)
p=0.2
p=0.5
p=1
p=5
p=10

(a)

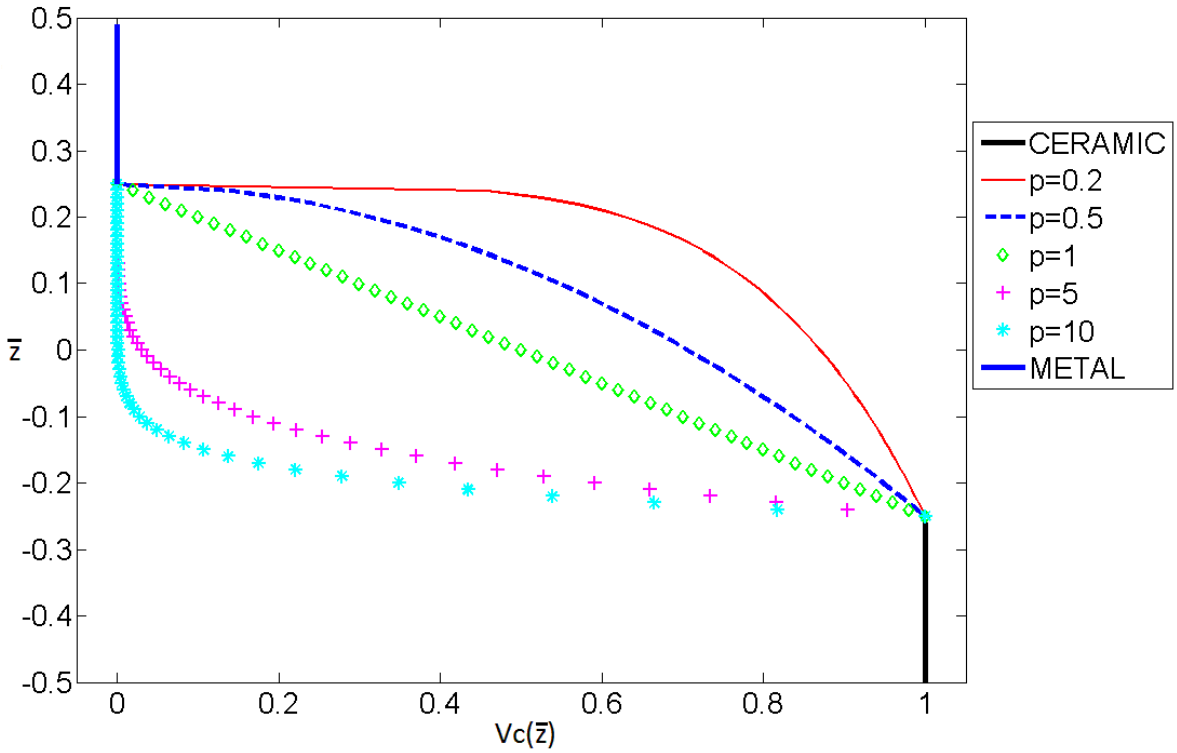
0.5
0.4
0.3
0.2
0.1
0
-0.1
-0.2
-0.3
-0.4
-0.5
z̄
0
0.2
0.4
0.6
0.8
1
Vc(z̄)
CERAMIC
p=0.2
p=0.5
p=1
p=5
p=10
METAL

(b)

Figure 3.

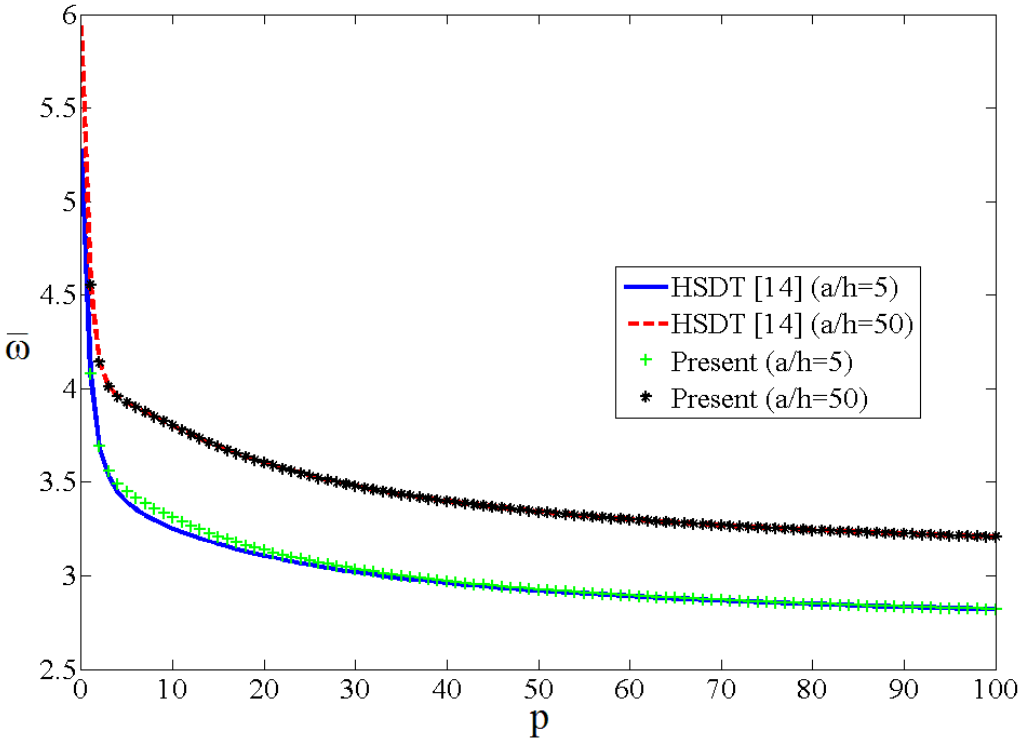
6
5.5
5
4.5
4
3.5
3
2.5
0
10
20
30
40
50
60
70
80
90
100
p
$\bar{\omega}$
HSDT [14] (a/h=5)
HSDT [14] (a/h=50)
Present (a/h=5)
Present (a/h=50)

Figure 4.

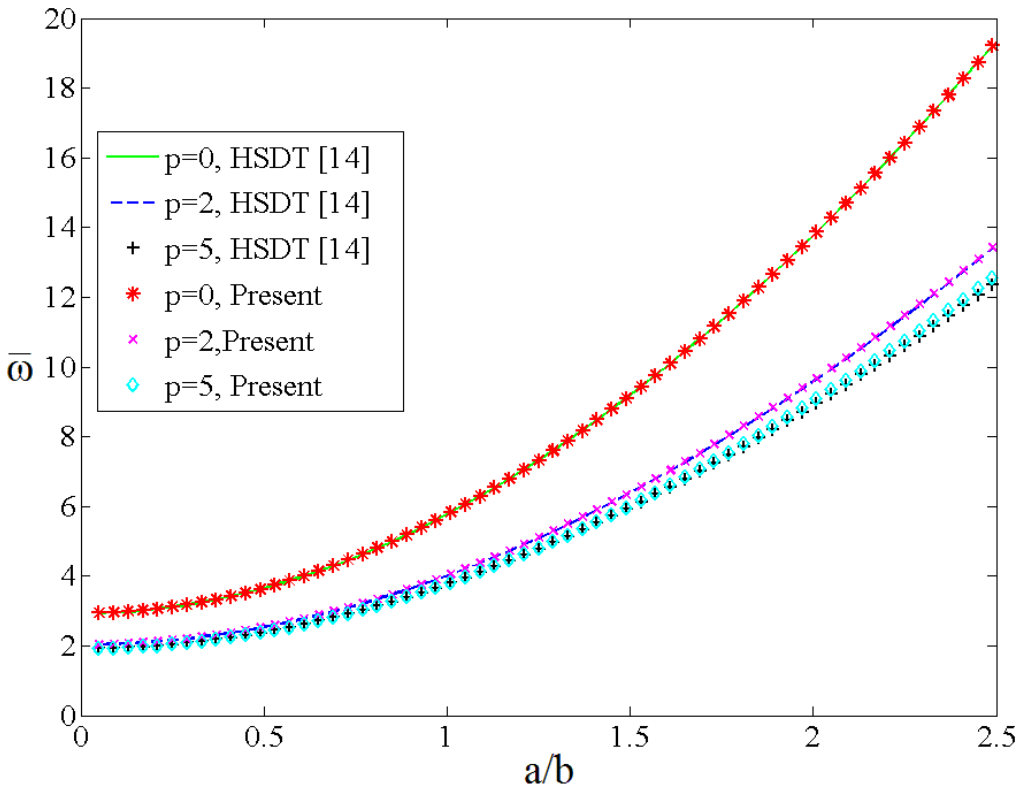
p=0, HSDT [14]
p=2, HSDT [14]
p=5, HSDT [14]
p=0, Present
p=2,Present
p=5, Present
$\bar{\omega}$
a/b
0
2
4
6
8
10
12
14
16
18
20
0
0.5
1
1.5
2
2.5